Acta Crystallographica Section F
Structural Biology and Crystallization Communications
ISSN 1744-3091

The structure of *Plasmodium vivax* phosphatidylethanolamine-binding protein suggests a functional motif containing a left-handed helix

Tracy Arakaki,[a,b] Helen Neely,[a,b] Erica Boni,[a,b] Natasha Mueller,[a,b] Frederick S. Buckner,[a,c] Wesley C. Van Voorhis,[a,c] Angela Lauricella,[a,d] George DeTitta,[a,d] Joseph Luft,[a,d] Wim G. J. Hol[a,e] and Ethan A. Merritt[a,b]*

[a]Structural Genomics of Pathogenic Protozoa (SGPP) Consortium, USA, [b]Department of Biochemistry, University of Washington, Seattle, WA 98195-7742, USA, [c]Department of Medicine, University of Washington, Seattle, WA 98195-7185, USA, [d]Hauptman–Woodward Institute, Buffalo, NY 14203, USA, and [e]Howard Hughes Medical Institute, University of Washington, Seattle, WA 98195, USA

Correspondence e-mail: merritt@u.washington.edu

Received 20 December 2006
Accepted 13 February 2007

PDB Reference: phosphatidylethanolamine-binding protein, 2gzq, r2gzqsf.

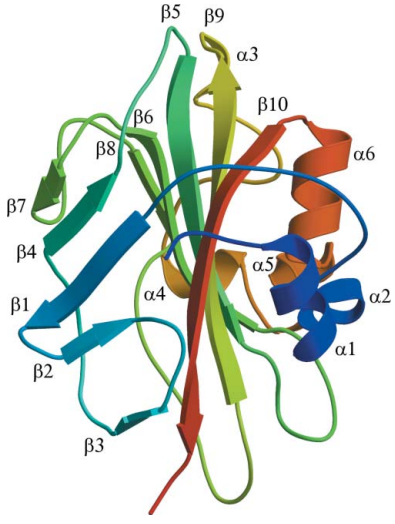

The structure of a putative Raf kinase inhibitor protein (RKIP) homolog from the eukaryotic parasite *Plasmodium vivax* has been studied to a resolution of 1.3 Å using multiple-wavelength anomalous diffraction at the Se *K* edge. This protozoan protein is topologically similar to previously studied members of the phosphatidylethanolamine-binding protein (PEBP) sequence family, but exhibits a distinctive left-handed α-helical region at one side of the canonical phospholipid-binding site. Re-examination of previously determined PEBP structures suggests that the *P. vivax* protein and yeast carboxypeptidase Y inhibitor may represent a structurally distinct subfamily of the diverse PEBP-sequence family.

1. Introduction

The eukaryotic parasite *Plasmodium* is the causative agent of malaria, affecting 2.1 billion people worldwide and, as of 1992, causing more than 1.2 million deaths annually (Pink *et al.*, 2005). Two species, *P. falciparum* and *P. vivax*, are responsible for most of the fatalities. Although vivax malaria is not as fatal as falciparum malaria, it has greater morbidity and has adverse effects on health, local economies and society (Mendis *et al.*, 2001). Vivax malaria is an acute and painful disease that, unlike falciparum malaria, may relapse owing to a unique characteristic of the life cycles of *P. vivax* and *P. ovale*: the generation of dormant hypnozoites in the liver (Sattabongkot *et al.*, 2004). Treatment for malaria includes sulfadoxine–pyrimethamine, chloroquine, pyrimethamine and mefloquine, but drug resistance to these drugs is a growing concern and new drugs are urgently needed (Maguire *et al.*, 2006; Schunk *et al.*, 2006). To address this need, the Structural Genomics of Pathogenic Protozoans consortium (SGPP; http://www.sgpp.org) sought to determine protein structures from major tropical eukaryotic pathogens, including *Plasmodium*. We report here the crystal structure of a Raf kinase inhibitor protein from *P. vivax* (TargetDB entry Pviv009166AAA, PlasmoDB genomic sequence Pv123630) at a resolution of 1.3 Å.

This protein is a member of the Pfam 'phosphatidylethanolamine-binding protein' (PEBP) sequence family PF01161. This family contains over 500 sequences, only a small number of which have been individually characterized as to specific biological function. Some PEBP-family members are known to be involved in membrane biogenesis (Hickox *et al.*, 2002) or to inhibit cell proliferation and differentiation (Yamazaki *et al.*, 2004). These biological roles could plausibly arise from the ability of this cytosolic protein to bind the head group of membrane-component phospholipids. However, other family members mediate diverse biological functions that are not obviously dependent on membrane binding. Some PEBPs inhibit NF-κB activation by interacting with NF-κB-inducing kinase (Yeung *et al.*, 2001) and other members of the family inhibit specific serine proteases (Hengst *et al.*, 2001; Mima *et al.*, 2005). Some mammalian PEBPs are known to bind Raf-1, inhibiting the phosphorylation of MEK1 by Raf-1 and disrupting interactions between Raf-1 and MEK (Yeung *et al.*, 1999). Consequently, these PEBPs inhibit the mitogen-activated protein kinase (MAPK) cascade initiated by Raf-1 and are also known by the name Raf kinase inhibitor proteins (RKIPs). Mutated forms of Raf are found in 30% of human cancers and thus RKIP is an attractive cancer drug target (Yamazaki *et al.*, 2004). The

Table 1
Data-collection and phasing statistics.

	Data set 1			Data set 2
Space group	$P2_12_12_1$			$P2_12_12_1$
Unit-cell parameters (Å)	a = 39.5, b = 54.5, c = 96.1			a = 39.3, b = 54.1, c = 94.4
Wavelength (Å)	0.9793	0.9795	0.9537	0.9794
Resolution (Å)	15.4–1.49 (1.57–1.49)	15.4–1.49 (1.57–1.49)	14.9–1.49 (1.57–1.49)	50–1.15 (1.19–1.15)
Total unique reflections	31377	31323	32500	69913
R_{sym}	0.04 (0.26)	0.04 (0.31)	0.04 (0.40)	0.097 (0.233)
Completeness (%)	100 (57)	100 (57)	100 (70)	96 (84)†
$I/\sigma(I)$	14.6 (2.6)	14.6 (2.6)	13.1 (2.2)	7.5 (2.9)
Redundancy	3.1 (1.6)	3.0 (1.6)	3.1 (1.7)	2.9 (1.9)
Wilson B factor (Å^2)	18	18	18	11
Phasing power‡ (dis/ano)	0/0.83	0.39/0.54	0.25/0.49	
Figure of merit	0.37 (0.59 after solvent flattening)			

† Observed data were 99% complete to a resolution of 1.3 Å. ‡ Phasing power = $(\sum|\Delta F_H|^2/\sum\varepsilon^2)^{1/2}$, where ΔF_H is either the dispersive or anomalous difference attributed to Se scattering.

P. falciparum RKIP homolog has been shown to affect autophosphorylation *versus* substrate phosphorylation by *P. falciparum* Ca-dependent protein kinase 1 (PfCDPK1) *in vitro* and has been suggested to play a corresponding regulatory role in the parasite (Kugelstadt *et al.*, 2007). The homologous *P. vivax* protein described here shares 74% identity with the *P. falciparum* sequence. Evaluation of the suitability of RKIP as a drug target in protozoa has not been previously reported.

2. Methods

2.1. Protein expression and purification

The gene encoding Pviv009166AAA was cloned, expressed and purified as described previously (Mehlin *et al.*, 2006; Arakaki *et al.*, 2006). The expression construct, BG1861, is a modified version of pET14b (Alexandrov *et al.*, 2004) that includes a noncleavable hexahistidine tag. The protein was expressed in *Escherichia coli* and purified using an Ni–NTA column and by gel filtration on a HiLoad Superdex 200 26/60 column (Amersham Pharmacia Biotech).

2.2. Protein crystallization

Purified protein was screened at the high-throughput facility at the Hauptman–Woodward Institute (Luft *et al.*, 2003) to identify initial crystallization conditions. The frozen sample [193 K, 13.2 mg ml^{-1} Pviv009166AAA, 500 m*M* NaCl, 0.025%(*w*/*v*) NaN_3, 5%(*v*/*v*) glycerol, 2 m*M* DTT, 25 m*M* HEPES pH 7.25] was rapidly thawed in a 303 K water bath prior to setup (Deng *et al.*, 2004). The sample was combined with 1536 distinct crystallization cocktails in ∼10 min in a single microassay plate (Greiner BioOne, 790801). After setup, each well of the plate held a unique microbatch-under-oil crystallization experiment (Chayen *et al.*, 1992) containing 200 nl sample combined with 200 nl crystallization cocktail under 5 µl USP-grade mineral oil (Sigma, catalog No. M-1180). The experiment plate was stored at 277 K for one week and then imaged at 296 K. Images were manually reviewed; 169 of the 1536 crystallization experiments produced outcomes that were suitable for optimization trials.

Initial hits were optimized and crystals were grown by the sitting-drop method. For native crystals, the crystallization drop consisted of 1 µl protein (8.6 mg ml^{-1}) mixed with 1 µl reservoir solution containing 8% PEG 8000, 40% PEG 400, 0.1 *M* HEPES (free acid) pH 7.5. Crystals of SeMet-incorporated protein grew under similar conditions except that the reservoir contained 0.04 *M* HEPES (free acid) pH 7.5 and 3.5 m*M* DTT.

Table 2
Refinement statistics.

Resolution (Å)	20–1.3
R	0.161
R_{free}	0.181
R.m.s.d. bonds (Å)	0.013
R.m.s.d. angles (°)	1.462
Protein atoms	1650
Nonprotein atoms	282
Residues in favored regions (%)	97.7
Residues in allowed regions (%)	100
TLS groups (residues)	1–23, 24–61, 62–69, 70–93, 94–101, 102–140, 141–151, 152–179
Mean (e.s.d.) B_{iso} + B_{TLS} protein atoms (Å^2)	15.5 (8.1)
Mean (e.s.d.) B_{iso} non-protein atoms (Å^2)	26.1 (8.9)

2.3. Data collection and structure determination

Data were collected at ALS beamline 8.2.2. Crystals were flash-frozen directly in liquid nitrogen. Data were collected from two crystals of SeMet-derivatized protein. One data set, collected for Se-edge MAD phasing, was processed and scaled using the automated protein-crystal structure-determination system *ELVES* (Holton & Alber, 2004). *SOLVE* (Terwilliger & Berendzen, 1999) found five Se sites and phases were submitted to *RESOLVE* for autobuilding (Terwilliger & Berendzen, 1999; Terwilliger, 2003). *RESOLVE* built 174 residues of 192 possible residues (not including the His tag). The remaining residues were built by hand using *Coot* (Emsley & Cowtan, 2004) and refined in *REFMAC*5 (Murshudov *et al.*, 1997). The structure was further refined using a second data set of higher resolution. This second data set was processed and scaled using *HKL*-2000 (Otwinowski & Minor, 1997). In the last three cycles of refinement, the protein chain was described by eight TLS groups identified by the TLSMD server (Painter & Merritt, 2006) and TLS parameters were refined for each group. Crystallographic statistics

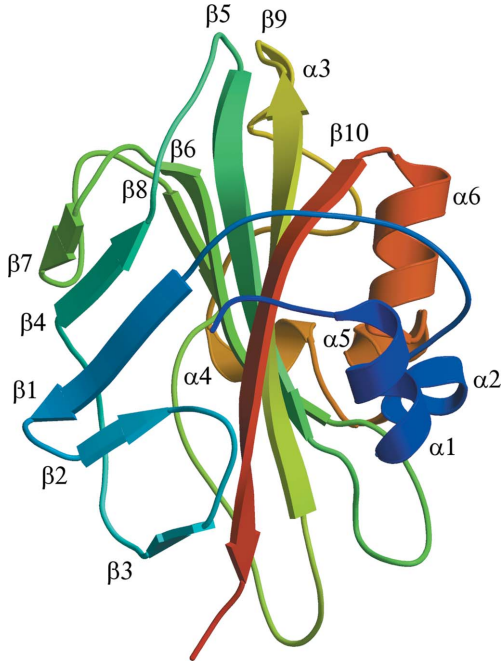

Figure 1
P. vivax Raf kinase inhibitor protein. The *P. vivax* protein exhibits the canonical PEBP fold: a central β-sheet flanked on one side by a second β-sheet at roughly 90° and on the other side by α-helices.

are presented in Tables 1 and 2. Waters were added using *Coot*. Model quality was validated using *Coot*, *PROCHECK* (Hooft *et al.*, 1996) and *MolProbity* (Lovell *et al.*, 2003). The final model consists of residues 2–192 of 191 expected residues. The additional residue is a result of a cloning artifact at the C-terminus whereby the chain ends with QMRRK rather than the target sequence QIEA.

3. Results and discussion

3.1. Overall structure

P. vivax RKIP has an overall $\alpha\beta$ fold with a large central β-sheet (Fig. 1). This general topology is shared by all structures from the PEBP-sequence family that have been determined to date. There are six helices in the *P. vivax* protein, α1 (6–13), α2 (14–19), α3 (142–144), α4 (155–159), α5 (162–167) and α6 (169–177), and there are ten strands, β1 (31–36), β2 (39–41), β3 (46–48), β4 (58–61), β5 (69–77), β6 (91–99), β7 (103–105), β8 (113–116), β9 (130–140) and β10 (180–190). The central β-sheet consists of strands β5, β6, β8, β9 and β10. The central sheet is flanked on one side by a second sheet comprised of the remaining five strands and on the other side by helices α1, α2 and α5. There are three *cis*-peptide bonds: Ile16-Pro17, Phe80-Pro81 and Arg89-Asp90. An equivalent nonproline *cis*-peptide is observed in other PEBP structures.

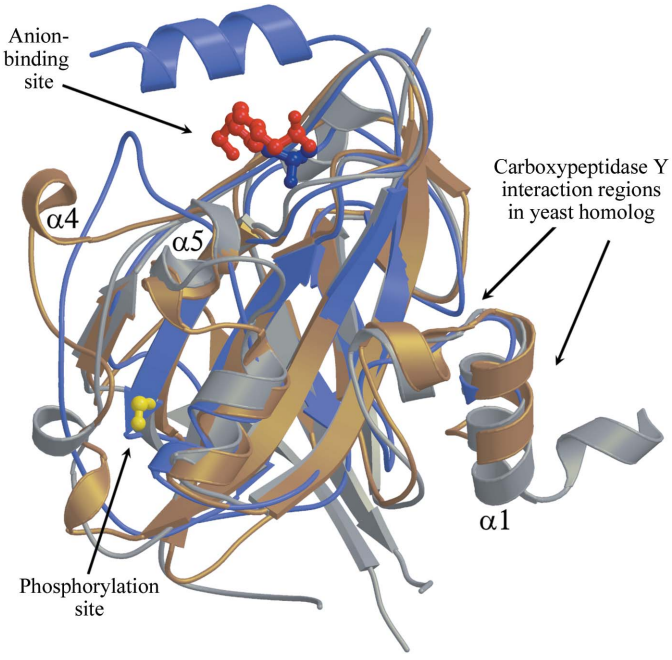

Figure 2
Structural superposition of three eukaryotic PEBPs. One monomer of the human RKIP with bound cacodylate (PDB code 1beh) is shown in blue. The HEPES molecule from the structure of one *E. coli* PEBP monomer (PDB code 1fjj) is shown in red, although the *E. coli* protein itself is omitted for clarity. The structure of yeast carboxypeptidase Y inhibitor (PDB code 1wpx) is shown in silver. The structure of the current *P. vivax* protein is shown in gold. Both cacodylate and HEPES bind at the anion-binding site characteristic of this protein family. The side chains of residues Val162 and Lys163 at one end of the left-handed α5 contribute to one face of the binding cavity and may serve to confer binding specificity. The anion-binding site in the human protein is more constrained than either the yeast, plasmodial or bacterial (not shown) sites. The extended binding site in mammalian proteins is bounded at one end by a loop that is spatially nearest to α4 in the *P. vivax* structure (far left of figure) and bounded at the top by a C-terminal helix that is not present in the other structures. This C-terminal extension is characteristic of mammalian PEBPs, but is not generally found in plant or bacterial homologs. The extended protein–protein interaction surface observed in the yeast inhibitor–carboxypeptidase complex corresponds to the right and rear of the protein in the orientation shown here. The N-terminus of the yeast PEBP (far right) occupies the active site of the peptidase (Mima *et al.*, 2005). The side chain of Ser97, the site of phosphorylation by PfCDPK1 in the plasmodial protein (Kugelstadt *et al.*, 2007), is shown in ball-and-stick representation (lower left). Superpositions were performed using *SSM* (Krissinel & Henrick, 2004).

3.2. Comparison with other phosphatidylethanolamine-binding proteins

P. vivax RKIP shares 20–25% sequence identity with various eukaryotic homologs and <20% identity with bacterial homologs. Pairwise structural superposition of the *P. vivax* protein against previously determined members of the PEBP-sequence family from six eukaryotic species (not including yeast) yielded r.m.s.d. values of 1.5–1.8 Å for 154 $\pm$ 5 C^{α} atoms. Superposition against bacterial homologs yielded r.m.s.d. values of 2.3–2.5 Å for 120 $\pm$ 4 C^{α} atoms. The closest structural homolog found was a eukaryotic PEBP, the yeast carboxypeptidase Y inhibitor, which yielded 1.5 Å r.m.s.d. for 170 C^{α} atoms. A structural superposition is shown in Fig. 2.

Structure-based sequence alignment of representative protozoan, mammalian, plant and bacterial PEBPs shows that the *P. vivax* sequence has several significant insertions relative to most eukaryotic homologs (Fig. 3). One of these, comprised of residues Asn165–Gln168 in the *P. vivax* sequence, is noteworthy in that it corresponds to the introduction of the structural element α5, a left-handed α-helix formed by residues 163–166 (Figs. 3 and 4).

Left-handed helices are rare; only 31 instances were found in 7284 structures surveyed from the PDB (Novotny & Kleywegt, 2005). As with other unusual structural features, they often appear on the protein surface at ligand-binding sites, protein–protein interfaces or other functional sites (Herzberg & Moult, 1991; MacArthur & Thornton, 1996). In the case of *P. vivax* PEBP, the left-handed helix α5 is located at one edge of the phospholipid-binding region, where it may play a role in the specific recognition of an unknown physiologically relevant presentation of the phosphatidylethanolamine head group at the membrane surface. As is apparent in Fig. 2, this distinctive structural feature is shared by the yeast carboxypeptidase Y inhibitor, although the presence of a left-handed helix in that protein was not previously remarked upon. The three-residue left-handed helical segment in the yeast structure was also not reported by the exhaustive automated survey of the PDB (Novotny & Kleywegt, 2005), as it was too short to meet the survey's criteria.

3.3. Functional implications

Notwithstanding its striking structural homology to the yeast protein in the region of α5, the *P. vivax* protein is unlikely to be a peptidase inhibitor. Binding of the yeast protein to carboxypeptidase Y is mediated by interaction surfaces on the opposite side of the protein (Figs. 2 and 3) and both inhibition and binding require the presence of the nonhomologous N-terminal extension (Mima *et al.*, 2005). However, the shared structural motif, including the left-handed helix, may indicate that the two proteins share a regulatory or recognition mechanism involving an interaction surface near the anion-binding site. Despite the nominal annotation of these proteins as phosphatidylethanolamine-binding proteins, it is not clear whether their normal biological role in fact involves membrane binding or whether the key interaction partner is another protein. The amino-acid side chains contributed by α5 to this interaction surface are hydrophobic and are consistent with either role. That is, they could help to stabilize association with a portion of the lipid tail distinct from the polar interactions that characterize the more highly conserved phosphatidylethanolamine end of the extended binding

site, or they could help to stabilize association with a partner protein that presents a complementary hydrophobic patch.

The *P. falciparum* PEBP is phosphorylated by PfCDPK1 at Ser96 (Ser97 in *P. vivax*; Kugelstadt *et al.*, 2007). This residue is shown by the present structure to lie on the same face of the protein as the anion-binding site, rather than the opposite face used by the yeast homolog to inhibit carboxypeptidase Y (Fig. 2).

Interference with RKIP-mediated signaling pathways in other eukaryotes has significant biological consequences (Trakul & Rosner, 2005; Eves *et al.*, 2006). Furthermore, the function of mammalian RKIPs may be disrupted with some specificity by drug-like molecules such as locostatin (Zhu *et al.*, 2005). Although not all PEBP homologues have been shown to belong to this class, Kugelstadt *et al.* (2007) have shown that the *P. falciparum* RKIP homolog is capable of modulating the activity of PfCDPK1, which is consistent with a function analogous to that of mammalian RKIPs.

4. Conclusions

The *P. vivax* phosphatidylethanolamine-binding protein, an RKIP homolog, is topologically similar to other structures from this large

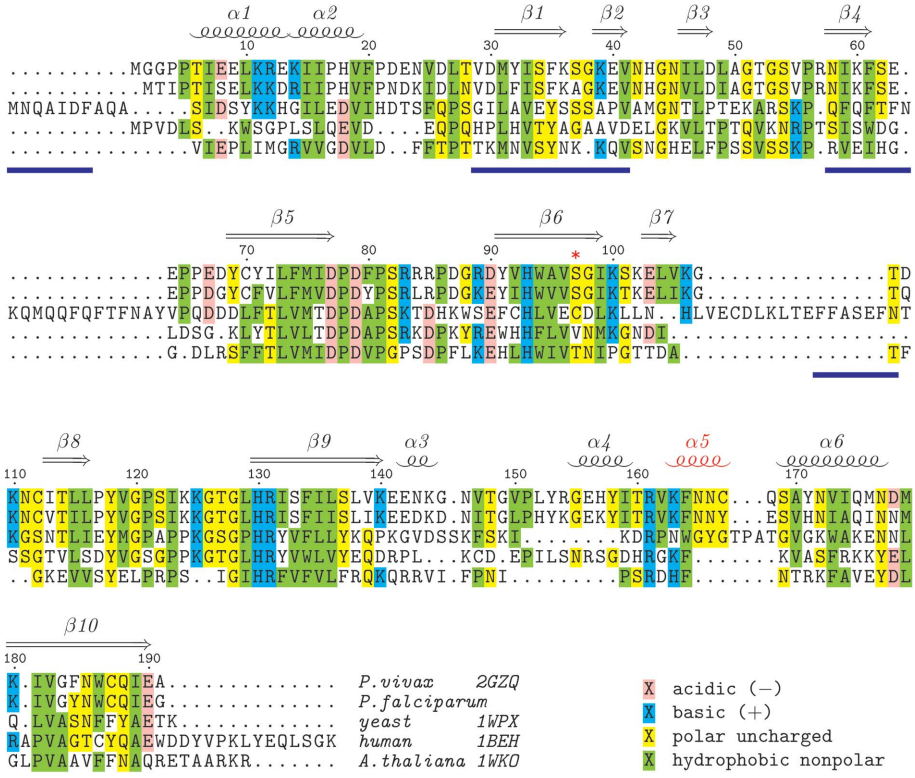

Figure 3
Structure-based sequence alignment of representative eukaryotic PEBPs. The structure-based sequence alignment of PEBPs from *P. vivax* (this structure), yeast (1wpx), human (1beh) and *Arabidopsis thaliana* (1wko) is shown. The *P. falciparum* sequence is aligned relative to the *P. vivax* sequence. The *P. falciparum* phosphorylation site is indicated by a red asterisk. Secondary-structural elements and residue numbers are shown for the *P. vivax* structure. The left-handed helix α5 found in *P. vivax* and yeast is indicated in red. The solid blue bars below the sequence indicate regions forming the protein–protein interface observed in the yeast complex of the PEBP with carboxypeptidase Y (Mima *et al.*, 2005). The C-terminal extension of the human protein is characteristic of mammalian PEBPs. Structural alignment was performed using the CE-MC server (Guda *et al.*, 2004). The figure was prepared with *TEXshade* (Beitz, 2000).

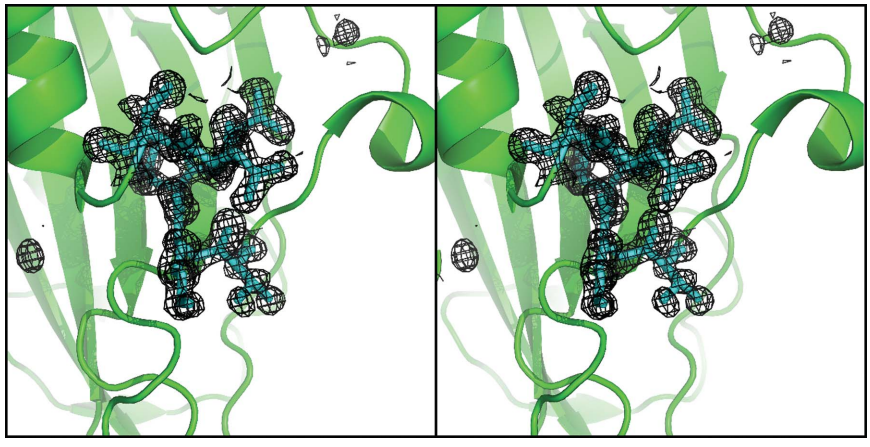

Figure 4
Electron density corresponding to the α5 left-handed helix. Density contours are drawn at a level of 1.25σ in a $2F_{obs} - F_{calc}$ map.

sequence family. However, it contains a distinctive structural motif, a left-handed α-helix at the canonical phospholipid-binding site, that is shared with only one previously characterized member of the family, the yeast carboxypeptidase Y inhibitor. This unusual shared structural feature appears to be relevant to the membrane-binding function of the protein rather than to recognition of a specific partner protein.

It would be helpful if additional members of the PEBP family could be identified that might belong to the same hypothetical functional subfamily, but this is difficult. The left-handed helix in both these proteins is formed from residues in a sequence insertion that is not present in most members of the PEBP-sequence family. However, there is no sequence identity between the *P. vivax* and yeast sequences in the respective inserts. If the shared structural motif indeed indicates that the two proteins are members of a functionally related subfamily of PEBP proteins, it is not clear that the other members of this subfamily can be identified purely by sequence comparison. Conversely, searches based on pre-identified structural motifs may also fail; for example, the homologous three-residue left-handed helix in the yeast carboxypeptidase inhibitor structure was too short to be flagged by an automated search of the PDB. The search turned up 600 candidate three-residue stretches based on φ/ψ angles, but not all were inspected manually and it is not clear how many of these are relevant (Novotny & Kleywegt, 2005). Better sequence-based methods of predicting propensity to form a left-handed helix might aid in such identification of possible functionally related subfamily members, but it seems likely that a combined sequence/structural approach will be needed.

We are grateful to Marian Novotny and Gerard Kleywegt for bringing the presence of the left-handed helix to our attention. We would like to thank Jonathan Caruthers and Isolde Le Trong for aid in data collection and crystal mounting. Financial support from the Protein Structure Initiative award NIGMS GM64655 and from NIH award AI067921 is gratefully acknowledged. Data collection was carried out at the Advanced Light Source, which is supported by the Director, Office of Science, Office of Basic Energy Sciences of the US Department of Energy under Contract No. DE-AC02-05CH11231.

References

Alexandrov, A., Vignali, M., LaCount, D. J., Quartley, E., de Vries, C., Rosa, D. D., Babulski, J., Mitchell, S. F., Schoenfeld, L. W., Fields, S., Hol, W. G., Dumont, M. E., Phizicky, E. M. & Grayhack, E. J. (2004). *Mol. Cell. Proteomics*, **3**, 934–938.

Arakaki, T., Le Trong, I., Phizicky, E., Quartley, E., DeTitta, G., Luft, J., Lauricella, A., Anderson, L., Kalyuzhniy, O., Worthey, E., Myler, P. J., Kim, D., Baker, D., Hol, W. G. J. & Merritt, E. A. (2006). *Acta Cryst.* F**62**, 175–179.

Beitz, E. (2000). *Bioinformatics*, **16**, 135–139.

Chayen, N. E., Shaw Stewart, P. D. & Blow, D. M. (1992). *J. Cryst. Growth*, **122**, 176–180.

Deng, J., Davies, D. R., Wisedchaisri, G., Wu, M., Hol, W. G. J. & Mehlin, C. (2004). *Acta Cryst.* D**60**, 203–204.

Emsley, P. & Cowtan, K. (2004). *Acta Cryst.* D**60**, 2126–2132.

Eves, E. M., Shapiro, P., Naik, K., Klein, U. R., Trakul, N. & Rosner, M. R. (2006). *Mol. Cell*, **23**, 561–574.

Guda, C., Lu, S., Scheeff, E. D., Bourne, P. E. & Shindyalov, I. N. (2004). *Nucleic Acids Res.* **32**, W100–W103.

Hengst, U., Albrecht, H., Hess, D. & Monard, D. (2001). *J. Biol. Chem.* **276**, 535–540.

Herzberg, O. & Moult, J. (1991). *Proteins*, **11**, 223–229.

Hickox, D. M., Gibbs, G., Morrison, J. R., Sebire, K., Edgar, K., Keah, H.-H., Alter, K., Loveland, K. L., Hearn, M. T. W., de Kretser, D. M. & O'Bryan, M. K. (2002). *Biol. Reprod.* **67**, 917–927.

Holton, J. & Alber, T. (2004). *Proc. Natl Acad. Sci. USA*, **101**, 1537–1542.

Hooft, R., Sander, C., Vriend, G. & Abola, E. (1996). *Nature (London)*, **381**, 272.

Krissinel, E. & Henrick, K. (2004). *Acta Cryst.* D**60**, 2256–2268.

Kugelstadt, D., Winter, D., Plückhahn, K., Lehmann, W. D. & Kappes, B. (2007). *Mol. Biochem. Parasitol.* **151**, 111–117.

Lovell, S. C., Davis, I. W., Arendall, W. B. III, de Bakker, P. I. W., Word, J. M., Prisant, M. G., Richardson, J. S. & Richardson, D. C. (2003). *Proteins*, **50**, 437–450.

Luft, J. R., Collins, R. J., Fehrman, N. A., Lauricella, A. M., Veatch, C. K. & DeTitta, G. T. (2003). *J. Struct. Biol.* **142**, 170–179.

MacArthur, M. W. & Thornton, J. M. (1996). *J. Mol. Biol.* **264**, 1180–1195.

Maguire, J. D., Marwoto, H., Richie, T. L., Fryauff, D. J. & Baird, J. K. (2006). *Clin. Infect. Dis.* **42**, 1067–1072.

Mehlin, C., Boni, E., Buckner, F. S., Engel, L., Feist, T., Gelb, M., Haji, L., Kim, D., Liu, C., Mueller, N., Myler, P. J., Reddy, J. T., Sampson, J. N., Subramanian, E., Van Voorhis, W. C., Worthey, E., Zucker, F. & Hol, W. G. J. (2006). *Mol. Biochem. Parasitol.* **148**, 144–160.

Mendis, K., Sina, B. J., Marchesini, P. & Carter, R. (2001). *Am. J. Trop. Med. Hyg.* **64**, *Suppl.* 1–2, 97–106.

Mima, J., Hayashida, M., Fujii, T., Narita, Y., Hayashi, R., Ueda, M. & Hata, Y. (2005). *J. Mol. Biol.* **346**, 1323–1334.

Murshudov, G. N., Vagin, A. A. & Dodson, E. J. (1997). *Acta Cryst.* D**53**, 240–255.

Novotny, M. & Kleywegt, G. J. (2005). *J. Mol. Biol.* **347**, 231–241.

Otwinowski, Z. & Minor, W. (1997). *Methods Enzymol.* **276**, 307–326.

Painter, J. & Merritt, E. A. (2006). *J. Appl. Cryst.* **39**, 109–111.

Pink, R., Hudson, A., Mouries, M.-A. & Bendig, M. (2005). *Nature Rev. Drug. Discov.* **4**, 727–740.

Sattabongkot, J., Tsuboi, T., Zollner, G. E., Sirichaisinthop, J. & Cui, L. (2004). *Trends Parasitol.* **20**, 192–198.

Schunk, M., Kumma, W. P., Miranda, I. B., Osman, M. E., Roewer, S., Alano, A., Loscher, T., Bienzle, U. & Mockenhaupt, F. P. (2006). *Malar. J.* **5**, 54.

Terwilliger, T. C. (2003). *Methods Enzymol.* **374**, 22–37.

Terwilliger, T. & Berendzen, J. (1999). *Acta Cryst.* D**55**, 849–861.

Trakul, N. & Rosner, M. R. (2005). *Cell Res.* **15**, 19–23.

Yamazaki, T., Nakano, H., Hayakari, M., Tanaka, M., Mayama, J. & Tsuchida, S. (2004). *J. Biol. Chem.* **279**, 32191–32195.

Yeung, K. C., Rose, D. W., Dhillon, A. S., Yaros, D., Gustafsson, M., Chatterjee, D., McFerran, B., Wyche, J., Kolch, W. & Sedivy, J. M. (2001). *Mol. Cell Biol.* **21**, 7207–7217.

Yeung, K., Seitz, T., Li, S., Janosch, P., McFerran, B., Kaiser, C., Fee, F., Katsanakis, K. D., Rose, D. W., Mischak, H., Sedivy, J. M. & Kolch, W. (1999). *Nature (London)*, **401**, 173–177.

Zhu, S., Henry, K. T. M., Lane, W. S. & Fenteany, G. (2005). *Chem. Biol.* **12**, 981–991.